I&EC research
Industrial & Engineering Chemistry Research

Article

pubs.acs.org/IECR

Chromate Reduction in Highly Alkaline Groundwater by Zerovalent Iron: Implications for Its Use in a Permeable Reactive Barrier

Samuel J. Fuller,[†] Douglas I. Stewart,*[,†] and Ian T. Burke[‡]

[†]School of Civil Engineering and [‡]School of Earth and Environment, University of Leeds, Leeds LS2 9JT, U.K.

Supporting Information

ABSTRACT: It is not currently known if the widely used reaction of zerovalent iron (ZVI) and Cr(VI) can be used in a permeable reactive barrier (PRB) to immobilize Cr leaching from hyperalkaline chromite ore processing residue (COPR). This study compares Cr(VI) removal from COPR leachate and chromate solution by ZVI at high pH. Cr(VI) removal occurs more rapidly from the chromate solution than from COPR leachate. The reaction is first order with respect to both [Cr(VI)] and the iron surface area, but iron surface reactivity is lost to the reaction. Buffering pH downward produces little change in the removal rate or the specific capacity of iron until acidic conditions are reached. SEM and XPS analyses confirm that reaction products accumulate on the iron surface in both liquors, but that other surface precipitates also form in COPR leachate. Leachate from highly alkaline COPR contains Ca, Si, and Al that precipitate on the iron surface and significantly reduce the specific capacity of iron to reduce Cr(VI). This study suggests that, although Cr(VI) reduction by ZVI will occur at hyperalkaline pH, other solutes present in COPR leachate will limit the design life of a PRB.

INTRODUCTION

Chromium is widely used in the chemical and metal alloy industries.[1−3] Historically most chromium has been obtained by the "high-lime" process, in which the Cr(III)-containing chromite ore is roasted with an alkali carbonate and limestone to produce soluble Cr(VI), which is then extracted with water upon cooling.[4,5] Large volumes of chromium ore processing residues (COPR) are produced,[5] which typically contain 2−7% chromium as a mixture of Cr(III) and Cr(VI) compounds.[6] Typical mineral phases include calcite, ettringite, hydrogarnet, and brownmillerite,[7] although the exact mineralogy depends on the initial processing mixture and whether constituents such as brownmillerite have undergone hydration reactions post processing.[7] Water in contact with high-lime COPR has a characteristically high pH 11.5−12,[6] and can contain up to 1.6 mmol·L^{-1} Cr(VI) as chromate.[8] Until recently COPR has been used as a fill material for roads and other construction projects,[4,6,9] or was dumped in unlined tips.[10−13] As a result, there are numerous sites around the world where water from COPR is contaminating the surrounding area with Cr(VI), which is a major concern as Cr(VI) is carcinogenic, mutagenic, and toxic.[14,15] Removal of COPR waste by traditional "dig and dump" remediation strategies is not only financially costly due to the large volumes of waste involved, but it is also inadvisable due to the risk of forming Cr(VI)-bearing dusts that are a confirmed human carcinogen through inhalation.[16] Thus remediation of COPR disposal sites will almost always involve two steps: placing a cover layer on the waste to prevent direct exposure and reduce rainwater infiltration, and treatment of any water that emerges from the waste.

A potentially cost-effective way to treat Cr(VI) contaminated groundwater is to construct a permeable reactive barrier (PRB) in the groundwater plume downstream of the waste.[17−19] In a PRB the contaminant is removed from solution as the groundwater flows through in a high permeability treatment zone created in the ground. Elemental iron (usually called zerovalent iron or ZVI) is a popular choice of reactive material where the contaminant can be treated by chemical reduction.[20,21] This is because iron oxidation is thermodynamically very favorable, and it can be coupled to the reduction of a range of industrial contaminants. ZVI is relatively low cost material that can be readily supplied in a range of particle sizes to match the permeability requirements of a particular application. A similar approach for Cr(VI) contaminated groundwater currently under development is to inject nanosized iron particles directly into the ground in order to create a reactive zone (so-called nano zerovalent iron, or nZVI, treatment).[22,23] Much work has already been done to investigate the use of ZVI and nZVI to reduce Cr(VI) over the common environmental pH range of mildly acidic to moderately alkaline conditions.[22−27] In acidic conditions the reaction is relatively fast, but the rate of reaction is slower in neutral and mildly alkaline conditions.[28]

The primary objective of this study is to extend understanding of the reaction between ZVI and Cr(VI) to alkaline conditions characteristic of COPR leachate. It reports on the rate of reaction between ZVI and Cr(VI) in hyperalkaline systems. It compares the behavior of a simple chromate solution with that of high-lime COPR leachate. Scanning electron microscopy (SEM) and X-ray photoelectron spectroscopy (XPS) on ZVI that has been exposed to each solution are presented. The effect of acidifying COPR leachate on ZVI reactivity is investigated, and the engineering implications for the use of ZVI in a PRB for highly alkaline COPR leachate are discussed.

Received: October 24, 2012
Revised: February 22, 2013
Accepted: March 2, 2013

   dx.doi.org/10.1021/ie302914b | *Ind. Eng. Chem. Res.* XXXX, XXX, XXX−XXX

BACKGROUND

Aerobic corrosion of the iron will rapidly consume any dissolved oxygen present in groundwater. Thus, within the majority of a ZVI PRB, iron will undergo anaerobic corrosion. The two half-reactions involved are[29]

$$Fe^{2+} + 2Fe^{-} \rightarrow Fe^{0} \qquad E^{\ominus} = -0.44\ V \tag{1}$$

$$2H_2O + 2e^{-} \rightarrow H_2 + 2OH^{-} \qquad E^{\ominus} = 0\ V \tag{2}$$

These combine to give the overall reaction:

$$Fe^{0} + 2H_2O \rightarrow Fe^{2+} + H_2 + 2OH^{-} \qquad E^{\ominus} = 0.44\ V \tag{3}$$

Anaerobic corrosion of elemental iron in water can produce aqueous ferrous ions at pH values below pH 9.[30] Above this value ferrous hydroxide, $Fe(OH)_2$, will form in reduced low temperature environments. $Fe(OH)_2$ is relatively stable in the short term[31] but can undergo a further transformation into magnetite, Fe_3O_4 (the Schikorr reaction[32]), or green rusts.[33] In weakly buffered systems reaction 3 results in an increase in pH which can limit the reaction due to the precipitation of corrosion products on the iron surface. If carbonate is present, Fe(II) can also precipitate as siderite ($FeCO_3$) or chukanovite ($Fe_2(OH)_2CO_3$).[34] Different corrosion products offer different degrees of protection to the iron surface (i.e., different degrees of passivation). For example, a surface layer of magnetite is prone to stress cracking and is therefore porous, exposing some of the iron surface beneath.[35]

The thermodynamic instability of Fe(0) in aqueous solution can drive the reduction of Cr(VI) to Cr(III). The reaction is[36]

$$Fe^{0} + CrO_4^{2-} + 4H_2O \rightarrow Cr(OH)_3 + Fe(OH)_3 + 2OH^{-} \qquad E^{\ominus} = 0.673\ V \tag{4}$$

The $E^{\ominus}$ value for eq 4 was calculated from thermodynamic data.[29] It should be noted that the $E^{\ominus}$ value for eq 4 assumes unit activity for OH^{-}, whereas the $E^{\ominus}$ values for eqs 1−3 assume unit activity for H^{+}.

The primary reaction product tends to be a mixed Cr(III)−Fe(III) hydroxide phase (a solid solution of the two compounds has a lower solution activity than the pure phases), although other phases such as Cr_2O_3 can also form.[25] Aqueous chromate is a widely used and very effective inhibitor of iron corrosion because the mixtures of ferric and chromic oxides and hydroxides produced are deposited at the reaction site.[37] Such inhibition is responsible for slower reaction rates between ZVI and Cr(VI) with increasing concentrations of Cr(VI) in solution.[36] Cr(VI) can also be reduced by the Fe(II) species produced by anaerobic corrosion discussed above, but the rate tends to be slower for both thermodynamic and stoichiometric reasons. These secondary reactions are important in systems where the iron surface has been passivated (i.e., where Fe(0) is no longer in direct contact with the solution).

If reaction 4 is an elementary reaction on the surface of the iron, then the initial rate equation would be expected to have the form

$$\frac{d[Cr(VI)]}{dt} = -k[Cr(VI)]^{\alpha}(A)^{\beta} \tag{5}$$

where k is the rate constant, $[Cr(VI)]$ is the concentration of Cr(VI), and A is the surface area of iron; α and β are the respective orders of reaction. In systems where the pH and amount of iron are effectively constant, this can be simplified to the pseudo rate equation

$$\frac{d[Cr(VI)]}{dt} = -k_{obs}[Cr(VI)]^{\alpha} \tag{6}$$

where $k_{obs} = k(A)^{\beta}$ and is the rate constant observed for such systems. Many researchers have used a rate equation of this format,[25,36,38−40] although there is some disagreement about the order of the rate equation with reported α values varying between 1[38−40] and 0.[36] This disparity is probably due to different test conditions employed, with different liquid:solid ratios and pH values affecting the value reported.

METHOD

Cr(VI) solution was made up from analytical grade potassium chromate (K_2CrO_4) (Fisher Scientific U.K. Ltd.) and deionized water that was deoxygenated by purging with N_2 for 30 min. The pH was adjusted with either HCl or NaOH. COPR leachate was obtained from a standpipe piezometer screened into COPR at a legacy COPR disposal site in the north of England (borehole 5; see ref 41 for details). The pH value of the COPR leachate was adjusted using HCl when required.

Iron metal fine filings (Fisher Scientific product code I/0850/50) were acid washed in 1 mol·L^{-1} HCl for 30 min, rinsed three times with deaerated, deionized water, and placed in 120 mL glass serum bottles (Wheaton Scientific, New Jersey, USA). Either chromate solution or COPR groundwater was added (100 mL), the headspace was purged with N_2, and the bottles were sealed with butyl rubber stoppers (Sigma-Aldrich Company Ltd., U.K.) and aluminum crimps (Kimble-Chase, USA). Solid solution ratios of 1−500 g·L^{-1} were used. The bottles were kept at the temperature 21 ± 1 °C. Periodically the bottles were sampled (2 mL) using nitrogen gas filled syringes and sterilized needles to maintain the oxygen-free headspaces. Samples were centrifuged for three minutes at 12000*g*, and the supernatant was decanted for analysis.

The particle size distribution of the iron filings was determined by dry sieving.[42] The pH value was determined using a Corning pH meter 240 with electrodes calibrated using standard pH 7 and 10 buffer solutions. Aqueous Cr(VI) concentration was determined by measuring the light absorption at 540 nm after reaction with diphenylcarbazide using a Thermo Scientific BioMate 3 UV/vis spectrophotometer (U.S. EPA method 7196A[43]). Major element concentrations were determined on a Perkin-Elmer 5300DV ICP-OES. Brunauer−Emmett−Teller (BET) analysis of the surface area of the ZVI granules was conducted using a Gemini V2365 system (Micromeritics Instrument Corp.) by the nitrogen adsorption method.[44]

Iron coupons (approximately 20 × 10 × 2 mm) were washed in 1 mol·L^{-1} HCl acid for 30 min with one set of coupons placed in a sealed 1 L bottle of COPR leachate with minimal headspace. A second set of coupons were placed in a sealed 1 L bottle of 1 mmol·L^{-1} chromate solution with minimal headspace (the solid solution ratio in these bottle tests was approximately 1 g·L^{-1} in order to minimize loss of Cr concentration with time). The iron coupons were exposed to the solutions for 2 months. Upon recovery coupons were rinsed in deionized water, dried by gentle patting with tissue paper, stored in dry tissue paper for approximately 1 h, and then mounted and carbon coated for scanning electron microscopy (SEM) analysis. A third set of acid washed iron coupons were

dx.doi.org/10.1021/ie302914b | Ind. Eng. Chem. Res. XXXX, XXX, XXX−XXX

Table 1. Chemical Composition of COPR Leachate

Na, mmol·L^{-1} (mg·L^{-1})	Mg, mmol·L^{-1}) (mg·L^{-1})	K, mmol·L^{-1} (mg·L^{-1})	Ca, mmol·L^{-1} (mg·L^{-1})	Al, mmol·L^{-1} (mg·L^{-1})	S, mmol·L^{-1} (mg·L^{-1})	Si, mmol·L^{-1} (mg·L^{-1})	Cr(VI), mmol·L^{-1} (mg·L^{-1})	pH
0.543 (12.5)	3.00 (73.0)	1.00 (39.1)	13.77 (552)	0.061 (1.65)	5.95 (191)	1.00 (28.1)	0.994 (51.7)	12.34

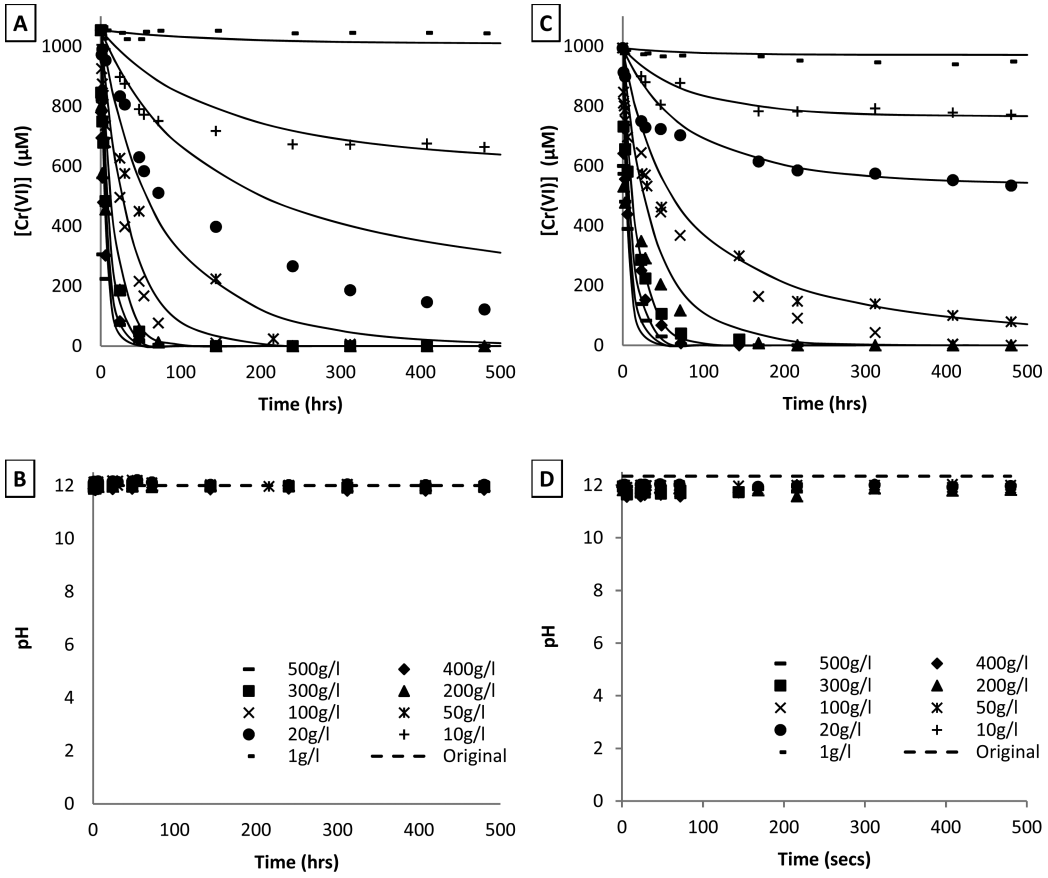

Figure 1. (A) Aqueous [Cr(VI)] vs time for tests with different solid solution ratios in chromate solution. (B) pH vs time for different solid solution ratios in chromate solution. (C) Aqueous [Cr(VI)] vs time for tests with different solid solution ratios in COPR leachate. (D) pH vs time for different solid solution ratios in COPR leachate.

prepared for SEM analysis without exposure to Cr(VI) solutions as controls. SEM analysis commenced 2.5 h after sample recovery, and was carried out on an FEI Quanta 650 FEG-ESEM. Energy dispersive X-ray spectra were collected with an Oxford X-max 80 SDD (liquid nitrogen free) EDS detector. Images were collected in secondary electron imaging mode.

Similar iron coupons, prepared the same way, were analyzed using X-ray photoelectron spectroscopy (XPS). These were removed from the test liquors 15 min before analysis and were dried using a nitrogen air line. XPS analysis was performed on a VG Escalab 250 with a high intensity monochromated Al Kα source.

RESULTS

Materials Characterization. The particle size distribution of the iron filings was very uniform with 95% of the particles between 75 and 300 μm. Their specific surface area after acid washing, determined by BET, was 0.28 m^2·g^{-1}. The COPR leachate had a pH of 12.3 and a Cr(VI) concentration of 994 μmol·L^{-1}. The chemical composition of the COPR leachate is reported in Table 1. The potassium chromate solution used for comparison with the COPR leachate was prepared with a pH of 12.0 and a Cr(VI) concentration of 1053 μmol·L^{-1}.

Effect of Solid Solution Ratio on Cr(VI) Removal Rates. Figure 1 shows the effect of ZVI on the aqueous Cr(VI) concentration in tests with chromate solution and COPR leachate at pH values of 12.0 ± 0.1 and 11.9 ± 0.2, respectively. Cr(VI) is removed from both solutions over time, with the time taken for complete Cr(VI) removal from solution increasing with decreasing solid to liquid ratio. In chromate solution, complete removal from the 50 g·L^{-1} test was achieved within about 15 days, whereas in the COPR leachate 92% removal had been achieved after 20 days. When the solid to liquid ratio was less than 50 g·L^{-1}, Cr(VI) removal was substantially incomplete after 20 days in both solutions. In all tests, the Cr(VI) removal rate was greatest at the start of the test and decreased steadily with time (the curves fitted to the data will be discussed later). At the same solid to liquid ratio Cr(VI) removal was slower in COPR leachate than in the chromate solution (for example, aqueous Cr(VI) was undetectable after 48 h in the 500 g·L^{-1} chromate solution test, whereas it took 72 h to reach the same point in the 500 g·L^{-1} COPR leachate test).

For each test the instantaneous rate of aqueous Cr(VI) removal associated with each time point has been estimated by

dx.doi.org/10.1021/ie302914b | Ind. Eng. Chem. Res. XXXX, XXX, XXX−XXX

fitting a quadratic equation through the preceding, current, and subsequent time points and differentiating that equation to determine the local gradient (data for time points where $[Cr(VI)]/[Cr(VI)]_0$ < 1% have been ignored). For the chromate solution tests there was an approximately linear relationship (r^2 > 0.91) between the logarithm of reaction rate and the logarithm of Cr(VI) concentration when the solid to liquid ratio was ≥100 g·L^{-1}. The average slope of the best-fit lines was 1.07 (standard deviation 0.16), indicating that the reaction is approximately first order with respect to the Cr(VI) concentration. There was also an approximately linear relationship (r^2 > 0.91) between the logarithm of reaction rate and the logarithm of Cr(VI) concentration for the COPR leachate tests when the solid to liquid ratio was ≥100 g·L^{-1}. The average slope of the best-fit lines for these tests was 1.16 (with a standard deviation of 0.19), indicating that the reaction is again roughly first order with respect to the Cr(VI) concentration. The 50 g·L^{-1} tests for both liquors also gave linear relationships that were roughly first order with respect to [Cr(VI)] although the data were more scattered (r^2 < 0.90). At solid solution ratios of <50 g·L^{-1} the log of the reaction rate against the log of the gradient for the chromate solution gave only roughly linear relationships with a lot of scatter (r^2 < 0.86) and slopes ≠ 1, indicating that all or part of these tests were not first order with respect to Cr(VI). Similarly, the COPR leachate data for solid solutions of <50g·L^{-1} showed scattered linear relationships (r^2 < 0.82) with slopes ≠ 1.

If the reaction is first order with respect to [Cr(VI)] at solid solution ratios of ≥100 g·L^{-1} (i.e., $\alpha = 1$ in eq 6), the integrated rate equation will have the form

$$[Cr(VI)] = [Cr(VI)]_0 e^{-k_{obs}t} \quad (7)$$

Thus k_{obs} has been estimated by fitting an exponential line to the data, ignoring the data points where $[Cr(VI)]/[Cr(VI)]_0$ < 1% (see Figure S1 in the Supporting Information). For both solutions k_{obs} increased approximately linearly with the solid to liquid ratio (see Figure 2), and the rate constant for the

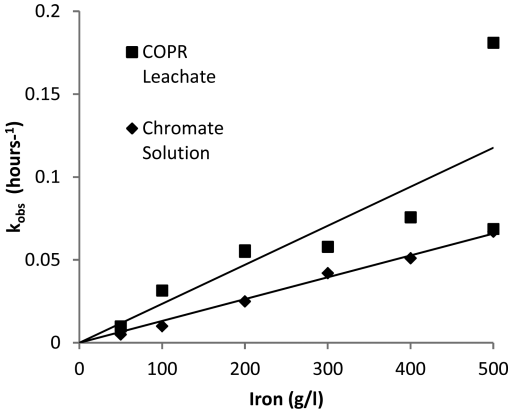

Figure 2. Variation in experimental first order rate constant, k_{obs}, with solid:liquid ratio (COPR leachate pH 11.9 ± 0.2, chromate solution pH 12.0 ± 0.1).

reaction of chromate solution with ZVI is approximately 50% higher than that for the reaction of COPR leachate with the same material. In those tests where the rate of Cr(VI) removal tended toward zero after 21 days without complete Cr(VI) removal from solution (solid to liquid ratios < 50 g·L^{-1}), the amount of Cr(VI) removed from solution increases approximately linearly with the amount of iron present, with the capacity of the iron in the chromate solution being about twice that in the COPR leachate (Figure 3). Linear relationships

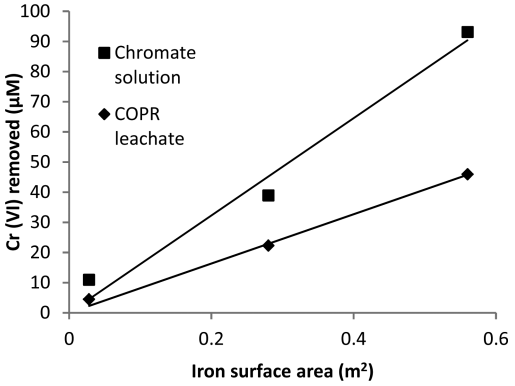

Figure 3. Variation in Cr(VI) reduction capacity of iron as a function of surface area for tests where the solid to liquid ratio is <50 g·L^{-1} (COPR leachate pH 11.9 ± 0.2, chromate solution pH 12.0 ± 0.1).

between both the experimental rate constant (at high solid to liquid ratios), and the Cr(VI) reducing capacity (at low solid to liquid ratios), and the amount of iron present suggest that iron availability is the limiting factor for the reduction reaction.

Effect of Initial pH on Cr(VI) Removal Rates. Figure 4 shows the removal of Cr(VI) from COPR leachate when the pH is buffered downward to different initial values. Tests were conducted with three solid to liquid ratios: 10, 20, and 100 g·L^{-1}. In all tests except those with an initial pH value of 12.0 (i.e., the unbuffered tests also shown in Figure 1), the pH value of the system was buffered upward with time. Typically the tests with higher solid to liquid ratios buffered to higher final pH values, and there is some evidence that buffering occurs more rapidly in these tests (although the data are not conclusive on this second point).

Cr(VI) was removed from solution at all initial pH values, at all three solid to liquid ratios, but only reached completion when the solid to liquid ratio was 100 g·L^{-1} or the initial pH value was 2 (the 20 g·L^{-1} test with an initial pH value of 4.0 was very close to completion after 20 days). The rate of reaction in the tests where the initial pH value was 2 was extremely high, and occurred before there was significant change in the pH value (the Cr(VI) concentration was below the detection limit after 6, 3, and 0.2 h in the 10, 20, and 100 g·L^{-1} tests, respectively). Otherwise, Cr(VI) removal was contemporaneous with the change of pH.

When the solid to liquid ratio was 100 g·L^{-1}, Cr(VI) was completely removed from solution at a rate that generally increased with decreasing initial pH value, although tests with initial pH values of 10.0, 9.0, 8.0, and 6.0 responded in quite similar manners, possibly because their pH values were rapidly buffered to comparable values. In this test series, then, there was a roughly linear relationship (with one exception, r^2 > 0.91) between the logarithm of reaction rate and the logarithm of Cr(VI) concentration over the range 12.0 ≥ pH ≥ 4.0 (in the pH 2 tests the reaction was more than 2 orders of magnitude faster than in the other tests and, as a result, the kinetics were not accurately captured by the approach taken in this study). The average slope of the best-fit lines was 1.12 (with a standard deviation of 0.13), indicating that the reaction is approximately first order with respect to the Cr(VI) concentration. k_{obs} values

dx.doi.org/10.1021/ie302914b | Ind. Eng. Chem. Res. XXXX, XXX, XXX−XXX

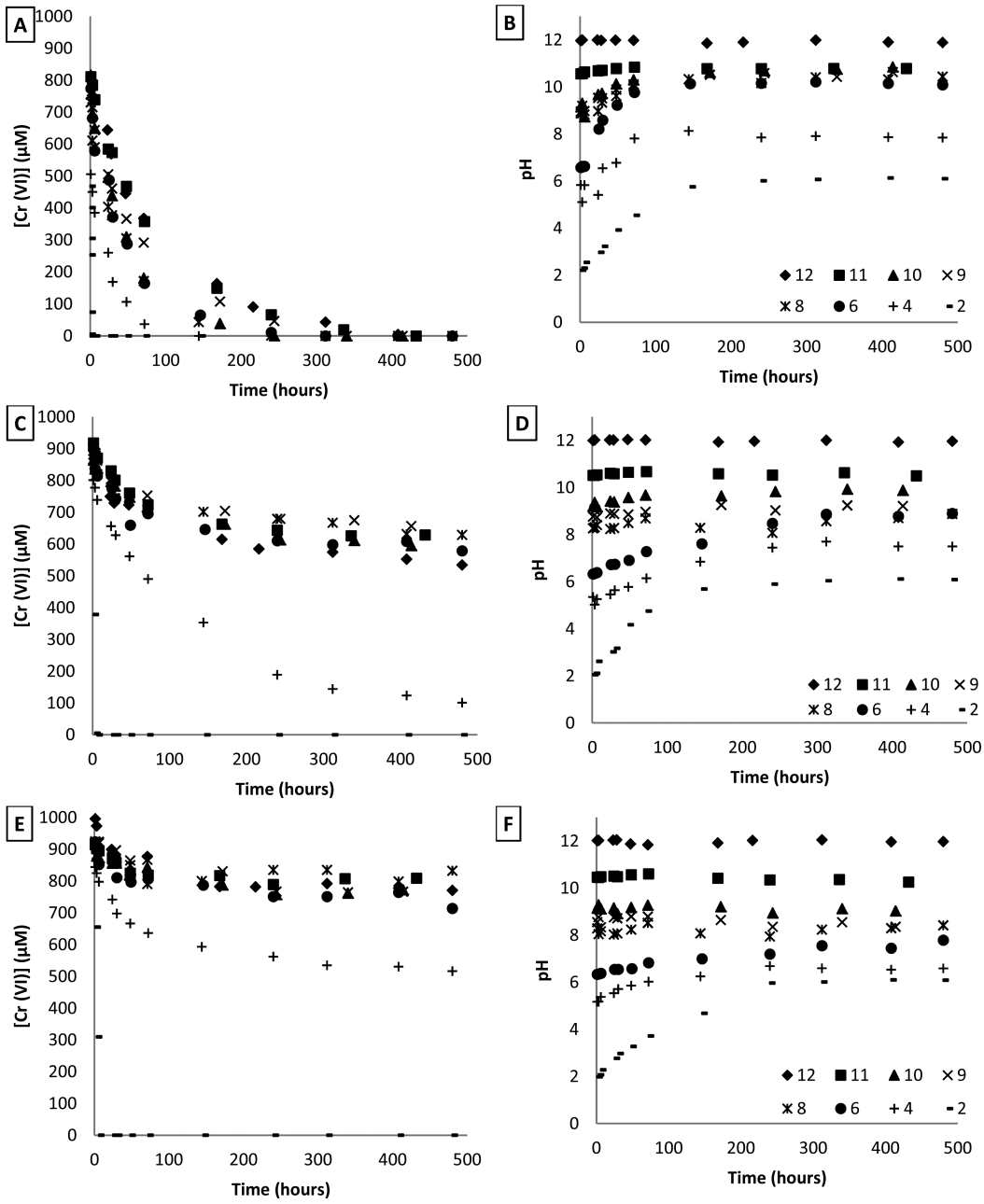

Figure 4. Variation of [Cr(VI)] and pH with time for COPR leachate buffered to different initial pH values: (A and B) solid solution ratio of 100 g·L^{-1}, (C and D) solid solution ratio of 20 g·L^{-1}, and (E and F) solid solution ratio of 10 g·L^{-1}.

estimated by fitting an exponential line to the data (Figure S2 in the Supporting Information) are shown in Figure 5 as a function of pH (as the pH increased during these tests, the value when $[Cr(VI)]/[Cr(VI)]_0$ = 50% is plotted in Figure 5). The value of k_{obs} decreases from about 0.04 to 0.01 h^{-1} as the initial pH increases from 4 to 12. A single trendline has not been fitted to the data in Figure 5 as it is likely that the reaction mechanism will vary with the pH value due to changes in the reactants, for example, chromate changing to hydrogen chromate or dichromate and Fe(II) becoming soluble at lower pH; however, it is clear that the reaction rate is relatively insensitive to pH in the alkaline region (it decreases by a factor of 2 as the pH value increases from 7 to 12).

SEM Analysis of Cr-Reacted ZVI Coupons. SEM images of an acid washed ZVI coupon and coupons exposed to K_2CrO_4 solution and COPR leachate (both containing ∼1 mmol·L^{-1} Cr(VI)) are shown in Figure 6. The unreacted sample was bright silvery gray in color to the naked eye. Figure 6A shows a typical SEM image of the acid washed coupon and corresponding EDS spectra, which contained Fe peaks only. The coupons exposed to K_2CrO_4 solution were a uniform dull gray color to the naked eye. Under the SEM the reacted surface was coated in a very thin speckled layer with EDS spot analysis containing weak Cr and O peaks in addition to prominent Fe peaks (Figure 6B). The iron coupons exposed to COPR were also a uniform dull gray color upon recovery. High magnification SEM analysis revealed a variable surface coating that contained Cr, Ca, S, Al, Si, and O in addition to Fe (Figure 6C). Lower magnification element maps (Figure 7) show three distinct types of surface coating were present, each with

dx.doi.org/10.1021/ie302914b | Ind. Eng. Chem. Res. XXXX, XXX, XXX−XXX

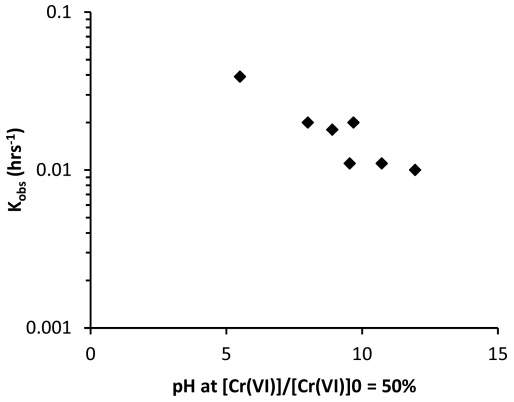

Figure 5. Variation in experimental rate constant k_{obs} with pH for COPR leachate when $[Cr(VI)]/[Cr(VI)]_0$ = 50% ($[Cr(VI)]_0$ = 1 mmol·L^{-1}; 100 g·L^{-1} iron).

different combinations of the observed elements. Some regions considerably richer in Ca, Si, and O show amorphous crystals, possibly a type of calcium silicate hydrate,[45] that form on top of the iron surface. Elongate prismatic crystals (approximately 5 × 1 × 1 μm) with Ca, S, Al, and O rich composition were also observed above the surface coating that have a morphology that is similar to ettringite.[46] Areas without any visible crystals had uniform EDS peaks of Cr, Fe, and O, similar to those seen in the chromate solution. The area of the iron coupon that has been element mapped was selected because the three characteristic surface structures were in close proximity.

XPS Analysis of Cr(VI) Reacted Coupons. XPS analysis of the coupon exposed to the chromate solution showed 85 ± 2% of the Cr present has a Cr $2p_{3/2}$ peak with a binding energy of 577.2 eV (Figure 8), consistent with a number of Cr(III) hydroxides.[47] The remaining 15 ± 2% of the Cr had a $2p_{3/2}$ peak with a binding energy of 579.2 eV, indicating Cr(VI). Three Fe peaks with binding energies of 706.9, 711.1, and 713.3 eV were detected, indicating the presence of elemental iron (5%) and two Fe(III) hydroxides (70 and 25%). There was a single O peak with a binding energy of 531.5 eV indicative of a hydroxide compound.[47]

XPS analysis of the coupon exposed to the COPR groundwater showed Cr $2p_{3/2}$ peaks with binding energies of 577.2 and 579.7 eV (Figure 8). Areas under the peaks indicated that 85 ± 2% was present as Cr(III) hydroxides, whereas 15 ± 2% was in the form of Cr(VI) (i.e., the same proportions as for the chromate solution). Fe peaks at 706.5, 710.5, and 713.3 eV showed iron to be either elemental or one of two hydroxides. Oxygen had peaks at 531.5 and 529.7 eV showing that 90% was in the form of a hydroxide whereas 10% was in the form of an oxide.[47]

DISCUSSION

Kinetics of Cr(VI) Reduction by ZVI under Hyperalkaline Conditions. At pH 12 the experimental rate constant, k_{obs}, that is obtained by fitting a simple first order rate equation (eq 7) to the data is directly proportional to the solid solution ratio when that ratio is ≥100 g·L^{-1} (see Figure 2). This strongly suggests that the rate of reaction is proportional to the iron surface area, and thus involves a surface reaction. This is not surprising as iron species have very low solubility above pH 9,[48] making a solution reaction unlikely.

The first step in any surface reaction is the sorption of the reactants onto the surface. In aqueous solution a hydroxylated

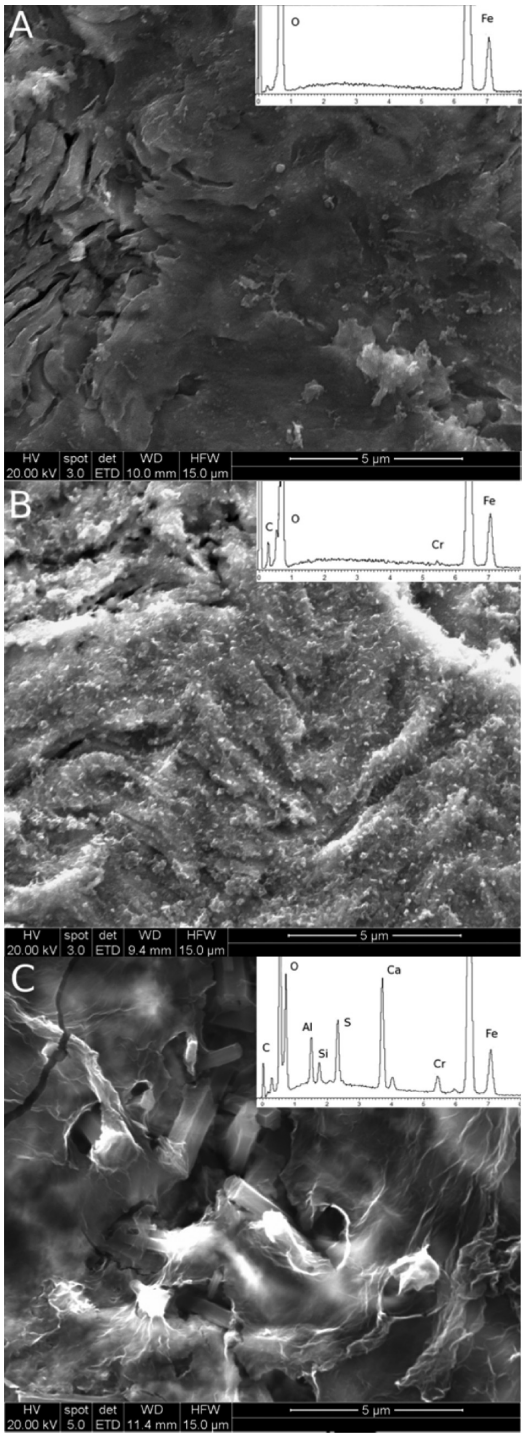

Figure 6. SEM images of iron surfaces with corresponding EDS spectra inserts exposed to (A) acid washed control specimen; (B) 1 mmol·L^{-1}, pH 12.0, Cr(VI) solution; and (C) 1 mmol·L^{-1}, pH 12.3, COPR leachate.

film immediately forms on the surface of elemental iron.[49,50] Some of these surface hydroxyls are exchangeable, and oxyanions, such as chromate, can form both monodentate surface complexes and biatomic−bidentate surface complexes where an oxygen is shared between the oxyanion and a surface iron atom.[51−53] The net surface charge of a hydoxylated iron surface is pH dependent (protons readily exchange with the surface groups to produce $-OH_2^+$, −OH, or $-O^-$ depending on pH).[50] For most iron-containing minerals, the solution pH

dx.doi.org/10.1021/ie302914b | Ind. Eng. Chem. Res. XXXX, XXX, XXX−XXX

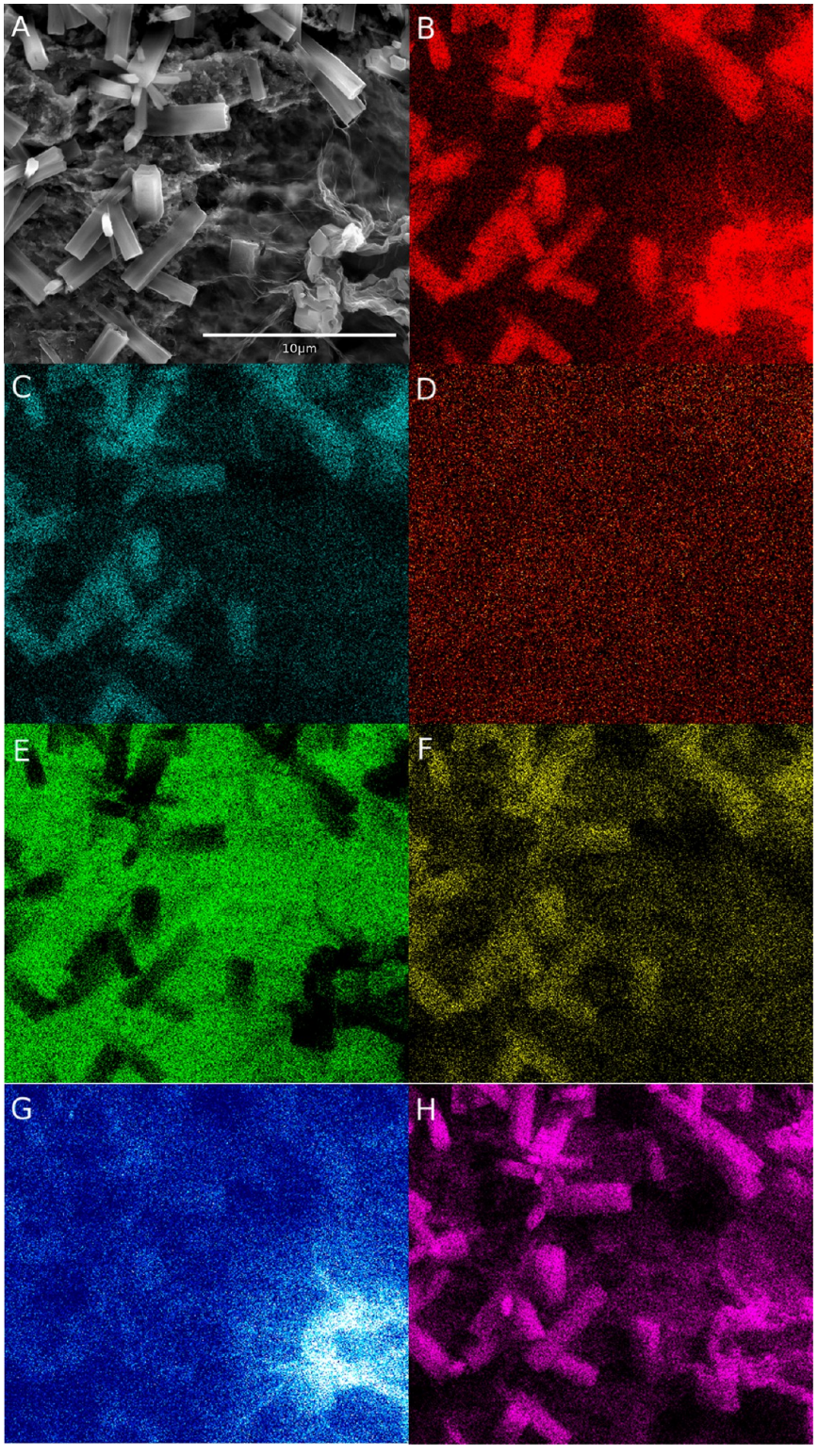

Figure 7. SEM image and EDS element mapping of iron surface exposed to 1 mmol·L^{-1}, pH 12.3, COPR leachate for 2 months. (A) Original SEM image; (B) calcium, (C) sulfur, (D) chromium, (E) iron, (F) aluminum, (G) silicon, and (H) oxygen.

value that results in no net charge on the surface (i.e., the point of zero charge, or pzc) is typically in the range pH 6−8.[54,55] Above the pzc, the net surface charge is negative, hindering the sorption of anionic species. Thus at pH 12 the amount of Cr(VI) retained by the surface by sorption is small,[51] and probably localized to edge sites and surface defects whose properties are less pH dependent. XPS analysis has confirmed that ≈15% of Cr associated with iron surfaces exposed to the hyperalkaline test liquors was the unreacted hexavalent form.

It has been widely reported that the removal of chromate from aqueous solution by elemental iron involves reduction of Cr(VI) to Cr(III).[25,56,57] The precise mechanism whereby a sorbed metal ion is reduced on a hydroxylated iron surface is poorly understood, but it has been found that reduction of

dx.doi.org/10.1021/ie302914b | Ind. Eng. Chem. Res. XXXX, XXX, XXX−XXX

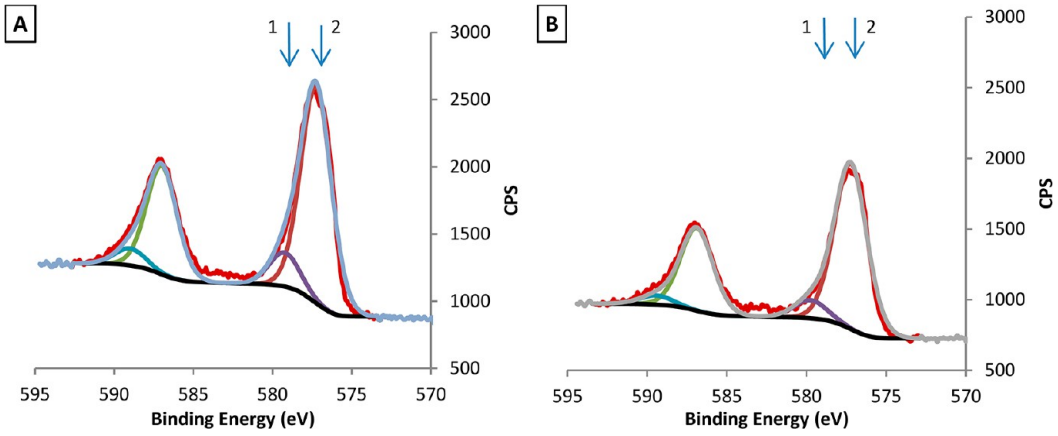

Figure 8. XPS curves showing chromium peaks for iron surface exposed to (A) 1 mmol·L^{-1}, pH 12.0, chromate solution and (B) 1 mmol·L^{-1}, pH 12.3, COPR leachate, for 2 months. ↓1, expected $2p_{3/2}$ peak position for Cr(VI) at 579 eV; ↓2, expected $2p_{3/2}$ peak position for Cr hydroxide at 577 eV.

metals tends to occur preferentially at surface defects, such as strained domain boundaries and cracks, that have intrinsically higher site reactivities.[53] Reduction of Cr(VI) coupled to the oxidation of Fe(0) is thermodynamically favorable even at high pH (reaction 4), so provided sorption at these edge sites is not inhibited by high pH, chromate sorption should be followed by reduction of Cr(VI) to Cr(III). XPS data (Figure 8) that showed that ≈85% of Cr present on the surface of the iron in both liquors tested is in the trivalent state supports this theory.

Studies of the sorption and reduction of U(VI) on ZVI have shown that adsorption is significantly faster than the subsequent reduction step.[50,53] Indeed most sorption studies investigating ZVI assume that sorption equilibrium is achieved in significantly less than 24 h.[52,58] Thus the data in Figure 1, which shows Cr(VI) removal over a period from about 2 to 20 days, strongly suggest that Cr(VI) sorption has time to reach equilibrium and that Cr(VI) reduction is the rate limiting step controlling the overall rate of Cr(VI) removal from solution. In such a system the rate at which individual sorbed species react with a surface is not directly influenced by the bulk solution concentration, but the overall reaction rate is a function of surface coverage. Site-specific sorption that can be described by a Langmuir isotherm results in surface coverage that is directly proportional to the solution concentration when overall surface coverage is low (i.e., when a species weakly sorbs). Thus, the overall rate equation is first order with respect to solution concentration.

When the solid to liquid ratio was less than 50 g·L^{-1} (see Figure 2), there was incomplete removal of Cr(VI) from solution, and the rate of reaction cannot be described by a simple first order rate equation. After 20 days, when the continuing rate of reaction was very small, the amount of Cr(VI) that was removed from solution was proportional to the amount of iron present. These low solid to liquid ratio tests suggest that an iron surface has a finite capacity for Cr(VI) reduction when the solution pH is high. SEM images of iron exposed to the chromate solution showed a speckled chromium-containing coating on the surface which the XPS data suggest is a mixed Fe(III)−Cr(III) hydroxide phase. It is therefore likely that the loss of reactivity is because the reaction products block the reactive sites on the iron surface. The problem with utilizing a rate equation that is first order with respect to [Cr(VI)], such as eq 7, is that it implies that Cr(VI) reduction will go to completion regardless of the initial solid solution ratio. If the reaction of Cr(VI) with ZVI is a surface reaction that is first order with respect to both [Cr(VI)] and surface area, A, then it would suggest a rate equation with the form

$$\frac{\mathrm{d}[\mathrm{Cr(VI)}]}{\mathrm{d}t} = -k_{12}[\mathrm{Cr(VI)}]A \tag{8}$$

where k_{12} is the area-corrected rate constant at pH 12 and has the units of m^{-2}·h^{-1}. If the only reason that reactive surface area is lost is due to the surface reaction of Cr(VI) with Fe(0), the surface area can be described by an equation of the form

$$A = A_0 - \frac{V}{B}([\mathrm{Cr(VI)}]_0 - [\mathrm{Cr(VI)}]) \tag{9}$$

where A_0 is the initial reactive surface area (m^2), B is the specific capacity of the iron surface to reduce Cr(VI) (mmol·m^{-2}), and V is the volume of liquid in contact with the iron (it is implicit that $A \geq 0$). Thus

$$\frac{\mathrm{d}[\mathrm{Cr(VI)}]}{\mathrm{d}t} = -k_{12}\frac{A_0}{r}[\mathrm{Cr(VI)}]\left(r - 1 + \frac{[\mathrm{Cr(VI)}]}{[\mathrm{Cr(VI)}]_0}\right) \tag{10}$$

where $r = A_0B/C_0V$ is the "capacity ratio" of the system (i.e., the ratio of the amount of Cr(VI) that can be reduced to the amount of Cr(VI) present). Equation 10 can be integrated (see the Supporting Information for the intermediate steps) to yield

$$\frac{[\mathrm{Cr(VI)}]}{[\mathrm{Cr(VI)}]_0} = \frac{(r-1)\exp\left[-k_{12}A_0\left(\frac{r-1}{r}\right)t\right]}{r - \exp\left[-k_{12}A_0\left(\frac{r-1}{r}\right)t\right]} = \frac{1-r}{1 - \left\{r\exp\left[-k_{12}A_0\left(\frac{1-r}{r}\right)t\right]\right\}} \tag{11}$$

Equation 11 satisfies the boundary conditions that [Cr(VI)] = [Cr(VI)]$_0$ when $t = 0$, and that either [Cr(VI)] → 0 as $t \to \infty$ when the capacity of the iron surface to reduce Cr(VI) exceeds the amount of Cr(VI) in solution (i.e., when $r > 1$) or [Cr(VI)] → $(1 - r)$[Cr(VI)]$_0$ as $t \to \infty$ when the amount of Cr(VI) in solution exceeds the capacity of the iron surface to reduce Cr(VI) (i.e., when $r < 1$). Further, when $r \gg 1$, eq 11 simplifies to [Cr(VI)]/[Cr(VI)]$_0$ ≈ exp[$-k_{12}A_0t$] (i.e., the variation of [Cr(VI)] with time can be described by a simple

dx.doi.org/10.1021/ie302914b | Ind. Eng. Chem. Res. XXXX, XXX, XXX−XXX

first order rate equation). Thus, at least qualitatively, eq 11 describes the observed behavior of the system.

Equation 11 has been used to draw the curves shown in Figure 1A. The specific capacity of the iron surface to reduce Cr(VI) at pH 12 has been estimated from Figure 3 and the value of k_{12} estimated by correcting the experimentally derived first order rate constants from the chromate solution tests with solid solution ratios of ≥100 g·L^{-1} (reported in Figure 2) for A_0 and $(r - 1)/r$.

For solid solution ratios of ≥100 g·L^{-1} eq 11 yields curves that appear to be first order and fit the data well. Below 100 g·L^{-1} eq 11 predicts the general pattern of behavior of behavior quite well, with an initially rapid removal of Cr(VI) from solution tailing off as the tests progress, although the initial rate of reaction is greater than is predicted. The total amount of Cr(VI) removed from the 20 g·L^{-1} test was also greater than predicted by eq 11. However, as small differences in the particle size distribution of the ZVI have disproportionately large effects on the surface area per unit weight of iron, the difference is not thought significant.

Effect of Solution Composition on Cr(VI) Reduction Rates. Comparing data from Figure 1A,C reveals that, for all solid solution ratios of ≥100 g·L^{-1}, complete removal of Cr(VI) occurs more quickly from the chromate solution than from the COPR leachate. Similarly, for all solid solution ratios of <100 g·L^{-1} the amount of Cr(VI) removed was always greater from the chromate solution (Figure 3). XPS data from both testing solutions showed that ≈85% of Cr Present on the iron surface was in the form of a Cr(III) hydroxide, and that part of the Fe is present as Fe(III) hydroxide (O is also present as hydroxide). This suggests that Cr reduction (reaction 4) results in precipitation of a mixed Fe(III)−Cr(III) hydroxide onto the iron surface which directly blocks the reaction site. SEM images of iron exposed to COPR leachate revealed that phases similar to ettringite and calcium silicate hydrate had been precipitated on a surface that was otherwise like the iron coupons exposed to a chromate solution. Thus it is believed that the reaction of Cr(VI) with the iron surface is inhibited not only by the reaction products from Cr(VI) reduction, but also by the reaction of other constituents of COPR leachate with the iron surface (SiO_3^- is reported to be an effective inhibitor of iron corrosion[59,60]). As a result, the iron surface has a lower capacity for Cr(VI) reduction.

It has been proposed that Cr(VI) reduction by elemental iron can be described by a two-step reaction: a fast sorption step that is in equilibrium, and a rate limiting reduction step. Where there is competition for reactive sites, it is reasonable to assume that there is a decrease in the number of reactive sites available for Cr(VI) sorption, but that the average time required to reduce a sorbed Cr(VI) molecule is unaffected. Equation 11 has therefore been used to produce the curves shown in Figure 1C by using a lower specific capacity for iron in contact with COPR leachate (estimated from Figure 3), but the same value for the area-corrected rate constant as used for modeling the behavior in chromate solutions. For solid solution ratios of ≤50 g·L^{-1} the removal curves are a good fit to the data (see Figure 1C), accurately predicting the amount of Cr(VI) removed before the reaction ceases. For solid solution ratios of >50g·L^{-1}, the curves slightly overpredict the initial rate at which Cr(VI) is removed from solution and thus give a slightly optimistic evaluation of when total removal will occur. This approach implicitly assumes that the impact of competing ions on Cr sorption in the first step of the reaction mechanism can be determined from the decrease in Cr reduction capacity. In reality, sorption equilibrium on reactive sites will reflect relative concentrations in solution, and thus will change over time if there are differences in the reaction rate of competing species. However, the small differences between the model and data suggest that the impact of this assumption is small and, thus, is a reasonable engineering approximation for the system studied.

The pH Dependence of Cr(VI) Reduction Rates. Over the pH range 7−12, the rate of Cr(VI) removal from COPR leachate was relatively insensitive to the pH value. For the 100 g·L^{-1} tests the first order rate constant decreased by only a factor of 2 as the OH^- concentration increased by a factor of 10^5 (Figure 5). In the 20 and 10 g·L^{-1} COPR leachate tests (where there was incomplete Cr(VI) removal), the specific capacity of the iron surface to remove Cr(VI) from solution did not vary significantly over this pH range. For Cr(VI) concentrations considered in this study, the dominant Cr(VI) species in aqueous solution at pH values above 5.9 is the chromate anion (CrO_4^{2-}),[61] and hydroxylated iron surfaces have a net negative surface charge in alkaline conditions,[54] restricting the sorption of anionic species to specific sites which remain available at high pH. Taken together, the lack of pH sensitivity of both the rate of reaction and the specific capacity of the iron surface suggest that the Cr(VI) is removed from solution by the same reaction mechanism across the pH range 7−12. The slight pH sensitivity of the rate of reaction probably reflects the slight increases in the activation energy of the reaction as the pH increases (the reaction constant for an elementary reaction is a function of the increase of Gibbs free energy that is required to form the reaction intermediate).

When the initial pH value was 4, the rate of Cr(VI) removal from COPR leachate was faster than in alkaline conditions (Figure 4). The first order rate constant determined for the 100 g·L^{-1} test (where there was complete Cr(VI) removal) was about twice the value at pH 7. The specific capacity of the iron determined in the 20 and 10 g·L^{-1} tests (where there was incomplete Cr(VI) removal) was 2−3 times greater than that in the alkaline range. Cr(VI) removal in the tests that started with a pH value of 2 was too fast for the rate constant to be quantified accurately, but the rate was orders of magnitude greater than in the higher pH tests. Also, there was complete Cr(VI) removal at all three solid to liquid ratios. Below pH 6 the dominant Cr(VI) species in aqueous solution is the hydrogen chromate anion ($HCrO_4^-$),[61] and hydroxylated iron surfaces have a net positive surface charge. As the reaction will involve a slightly different Cr(VI) species interacting with a differently charged surface, and the evidence is that the specific capacity of the surface is substantially higher, it seems reasonable to infer that the reaction mechanism in acid conditions is different from that in alkaline systems, although this study was not focused on acidic systems.

Engineering Implications. ZVI barriers have been deployed at several field sites where the groundwater pH is initially mildly alkaline without reported problems.[62,63] The data presented in this paper suggest that the use of ZVI to treat Cr(VI) contaminated groundwater could also be successful at more alkaline pH values provided the water does not contain solutes that compete with Cr(VI) for the reactive sites on the iron. As many soils contain silicates which become increasingly soluble above about pH 9.5,[48] this pH value may represent the upper pH limit at which iron can be deployed in a conventionally designed PRB.

dx.doi.org/10.1021/ie302914b | Ind. Eng. Chem. Res. XXXX, XXX, XXX−XXX

Solutes in COPR leachate slow the reaction of Cr(VI) with iron and significantly reduce the specific capacity of the iron surface. The implications for using iron as the reactive media within a PRB are that longer residence times will be required and that effective barrier thickness will be lost more quickly due to passivation of the iron. Thus significantly thicker barriers will be required to treat COPR leachate than would otherwise be required with groundwater contaminated with Cr. There is probably no engineering reason why a thicker reactive zone should not be used within a PRB, but this will impact the overall cost of the barrier, and may make such a solution uneconomical.

CONCLUSIONS

The rate at which Cr(VI) is removed from aqueous solution by reaction with elemental iron is independent of pH over the range 7−12. In this range the reaction is first order with respect to both [Cr(VI)] and the iron surface area. Iron surface reactivity is lost to the reaction, but the specific capacity of iron to reduce Cr(VI) is relatively independent of pH over the same range. As the reactive Cr(VI) species and the surface properties of iron do not vary significantly over this pH range, the pH independence of the reaction rate and specific capacity suggest that the reaction mechanism is the same from pH 7 to pH 12. Leachate from highly alkaline COPR contains solutes that significantly reduce the specific capacity of iron to reduce Cr(VI), probably because the solutes (e.g., silicate) compete with Cr(VI) for reactive sites on the iron.

ASSOCIATED CONTENT

Supporting Information

The full derivation of the integrated rate equation for Cr(VI) reduction by ZVI and logarithmic plots of [Cr(VI)] against time for COPR leachate and Cr(VI) solution at different solid solution ratios, and logarithmic plots of [Cr(VI)] against time for COPR buffered to different initial pH values. This material is available free of charge via the Internet at http://pubs.acs.org.

AUTHOR INFORMATION

Corresponding Author

*E-mail: d.i.stewart@leeds.ac.uk.

Notes

The authors declare no competing financial interest.

ACKNOWLEDGMENTS

S.J.F. would like to acknowledge his funding from a John Henry Garner Scholarship at the University of Leeds. The authors would like to thank Dr. Eric Condliffe and Dr. Benjamin Johnson for help and advice with the SEM and XPS work, respectively. They would like to acknowledge the Leeds EPSRC Nanoscience and Nanotechnology Research Equipment Facility for access to XPS. The authors would also like to thank Dr. Phil Studds and Mark Bell, Ramboll U.K., for help in obtaining COPR leachate.

REFERENCES

(1) Wang, Y. T. Microbial reduction of chromate. In *Environmental Microbe-Metal Interactions*; Lovley, D. R., Ed.; ASM Press: Washington, DC, 2000; pp 225−235.

(2) Jacobs, J. A.; Testa, S. M. Overview of chromium(VI) in the environment: Background and history. In *Chromium(VI) Handbook*; Guertin, E. J., Jacobs, J. A., Avakian, C. P., Eds.; CRC Press: Boca Raton, FL, 2005.

(3) Morales-Barrera, L.; Cristiani-Urbina, E. Hexavalent Chromium Removal by a Trichoderma inhamatum Fungal Strain Isolated from Tannery Effluent. *Water, Air, Soil Pollut.* **2008**, *187* (1), 327−336.

(4) Burke, T. Chromite Ore Processing Residue in Hudson County, New Jersey. *Environ. Health Perspect.* **1991**, *92*, 131−137.

(5) Darrie, G. Commercial Extraction Technology and Process Waste Disposal in the Manufacture of Chromium Chemicals from Ore. *Environ. Geochem. Health* **2001**, *23*, 187−193.

(6) Geelhoed, J. S.; Meeussen, J. C. L.; Hillier, S.; Lumsdon, D. G.; Thomas, R. P.; Farmer, J. G.; Paterson, E. Identification and geochemical modeling of processes controlling leaching of Cr(VI) and other major elements from chromite ore processing residue. *Geochim. Cosmochim. Acta* **2002**, *66* (22), 3927−3942.

(7) Chrysochoou, M.; Dermatas, D.; Grubb, D.; Moon, D.; Christodoulatos, C. Importance of Mineralogy in the Geoenvironmental Characterization and Treatment of Chromite Ore Processing Residue. *J. Geotech. Geoenviron. Eng.* **2010**, *136* (3), 510−521.

(8) Farmer, J. G.; Thomas, R. P.; Graham, M. C.; Geelhoed, J. S.; Lumsdon, D. G.; Paterson, E. Chromium speciation and fractionation in ground and surface waters in the vicinity of chromite ore processing residue disposal sites. *J. Environ. Monit.* **2002**, *4* (2), 235−243.

(9) Higgins, T. E.; Halloran, A. R.; Dobbins, M. E.; Pittignano, A. J. In situ reduction of hexavalent chromium in alkaline soils enriched with chromite ore processing residue. *J. Air Waste Manage. Assoc.* **1998**, *48* (11), 1100−1106.

(10) Breeze, V. G. Land Reclamation and River Pollution Problems in the Croal Valley Caused by Waste from Chromate Manufacture. *J. Appl. Ecol.* **1973**, *10* (2), 513−525.

(11) Jeyasingh, J.; Philip, L. Bioremediation of chromium contaminated soil: Optimization of operating parameters under laboratory conditions. *J. Hazard. Mater.* **2005**, *118* (1−3), 113−120.

(12) Stewart, D. I.; Burke, I. T.; Hughes-Berry, D. V.; Whittleston, R. A. Microbially mediated chromate reduction in soil contaminated by highly alkaline leachate from chromium containing waste. *Ecol. Eng.* **2010**, *36* (2), 211−221.

(13) Stewart, D. I.; Burke, I. T.; Mortimer, R. J. G. Stimulation of Microbially Mediated Chromate Reduction in Alkaline Soil-Water Systems. *Geomicrobiol. J.* **2007**, *24* (7), 655−669.

(14) Richard, F. C.; Bourg, A. C. M. Aqueous geochemistry of chromium: A review. *Water Res.* **1991**, *25* (7), 807−816.

(15) Fendorf, S. E. Surface reactions of chromium in soils and waters. *Geoderma* **1995**, *67* (1−2), 55−71.

(16) U.S. EPA. *Toxicological Review of Hexavalent Chromium*; 1998.

(17) Blowes, D. W.; Ptacek, C. J.; Benner, S. G.; McRae, C. W. T.; Bennett, T. A.; Puls, R. W. Treatment of inorganic contaminants using permeable reactive barriers. *J. Contam. Hydrol.* **2000**, *45* (1−2), 123−137.

(18) Gillham, R. W.; O'Hannesin, S. F. Enhanced Degradation of Halogenated Aliphatics by Zero-Valent Iron. *Ground Water* **1994**, *32* (6), 958−967.

(19) Starr, R. C.; Cherry, J. A. In Situ Remediation of Contaminated Ground Water: The Funnel-and-Gate System. *Ground Water* **1994**, *32* (3), 465−476.

(20) Alowitz, M. J.; Scherer, M. M. Kinetics of nitrate, nitrite, and Cr(VI) reduction by iron metal. *Environ. Sci. Technol.* **2002**, *36* (3), 299−306.

(21) Cantrell, K. J.; Kaplan, D. I.; Wietsma, T. W. Zero-Valent Iron For The In-situ Remediation Of Selected Metals In Groundwater. *J. Hazard. Mater.* **1995**, *42* (2), 201−212.

(22) Du, J.; Lu, J.; Wu, Q.; Jing, C. Reduction and immobilization of chromate in chromite ore processing residue with nanoscale zero-valent iron. *J. Hazard. Mater.* **2012**, *215−216*, 152−158.

(23) Chrysochoou, M.; Johnston, C. P.; Dahal, G. A comparative evaluation of hexavalent chromium treatment in contaminated soil by calcium polysulfide and green-tea nanoscale zero-valent iron. *J. Hazard. Mater.* **2012**, *201−202*, 33−42.

(24) Lee, T.; Lim, H.; Lee, Y.; Park, J.-W. Use of waste iron metal for removal of Cr(VI) from water. *Chemosphere* **2003**, *53* (5), 479−485.

(25) Cantrell, K. J.; Kaplan, D. I.; Wietsma, T. W. Zero-valent iron for the in situ remediation of selected metals in groundwater. *J. Hazard. Mater.* **1995**, *42* (2), 201−212.
(26) Franco, D.; Da Silva, L.; Jardim, W. Reduction of Hexavalent Chromium in Soil and Ground Water Using Zero-Valent Iron Under Batch and Semi-Batch Conditions. *Water, Air, Soil Pollut.* **2009**, *197* (1), 49−60.
(27) Powell, R. M.; Puls, R. W.; Hightower, S. K.; Sabatini, D. A. Coupled Iron Corrosion and Chromate Reduction: Mechanisms for Subsurface Remediation. *Environ. Sci. Technol.* **1995**, *29* (8), 1913−1922.
(28) Chang, L.-Y. Chromate reduction in wastewater at different pH levels using thin iron wires—A laboratory study. *Environ. Prog.* **2005**, *24* (3), 305−316.
(29) Stumm, W.; Morgan, J. J. *Aquatic Chemistry: Chemical Equilibria and Rates in Natural Waters*; Wiley: New York, 1996.
(30) Matheson, L. J.; Tratnyek, P. G. Reductive Dehalogenation of Chlorinated Methanes by Iron Metal. Environ. *Sci. Technol.* **1994**, *28* (12), 2045−2053.
(31) Roh, Y.; Lee, S. Y.; Elless, M. P. Characterization of corrosion products in the permeable reactive barriers. *Environ. Geol. (Heidelberg, Ger.)* **2000**, *40* (1/2), 184−194.
(32) Odziemkowski, M. S.; Schuhmacher, T. T.; Gillham, R. W.; Reardon, E. J. Mechanism of oxide film formation on iron in simulating groundwater solutions: Raman spectroscopic studies. *Corros. Sci.* **1998**, *40* (2−3), 371−389.
(33) Drissi, S. H.; Refait, P.; Abdelmoula, M.; Génin, J. M. R. The preparation and thermodynamic properties of Fe(II)/Fe(III) hydroxide-carbonate (green rust 1); Pourbaix diagram of iron in carbonate-containing aqueous media. *Corros. Sci.* **1995**, *37* (12), 2025−2041.
(34) Lee, T. R.; Wilkin, R. T. Iron hydroxy carbonate formation in zerovalent iron permeable reactive barriers: Characterization and evaluation of phase stability. *J. Contam. Hydrol.* **2010**, *116* (1−4), 47−57.
(35) Castle, J. E.; Mann, G. M. W. The mechanism of formation of a porous oxide film on steel. *Corros. Sci.* **1966**, *6* (6), 253−262.
(36) Melitas, N.; Chuffe-Moscoso, O.; Farrell, J. Kinetics of Soluble Chromium Removal from Contaminated Water by Zerovalent Iron Media: Corrosion Inhibition and Passive Oxide Effects. *Environ. Sci. Technol.* **2001**, *35* (19), 3948−3953.
(37) Evans, U. R.; Winterbottom, A. B. *Metallic Corrosion, Passivity and Protection*; E. Arnold and Co.: London, 1948.
(38) Gould, J. P. The kinetics of hexavalent chromium reduction by metallic iron. *Water Res.* **1982**, *16* (6), 871−877.
(39) Qian, H.; Wu, Y.; Liu, Y.; Xu, X. Kinetics of hexavalent chromium reduction by iron metal. *Front. Environ. Sci. Eng. China* **2008**, *2* (1), 51−56.
(40) Gheju, M.; Iovi, A. Kinetics of hexavalent chromium reduction by scrap iron. *J. Hazard. Mater.* **2006**, *135* (1−3), 66−73.
(41) Whittleston, R. A.; Stewart, D. I.; Mortimer, R. J. G.; Tilt, Z. C.; Brown, A. P.; Geraki, K.; Burke, I. T. Chromate reduction in Fe(II)-containing soil affected by hyperalkaline leachate from chromite ore processing residue. *J. Hazard. Mater.* **2011**, *194*, 15−23.
(42) British Standards Institution. *BS 1377-2:1990 Methods of Test for Soils for Civil Engineering Purposes. Classification Tests*; BSI: London, 1990.
(43) U.S. EPA. *SW-846 Manual: Method 7196A. Chromium Hexavalent (Colorimetric)*; 1992.
(44) Brunauer, S.; Emmett, P. H.; Teller, E. Adsorption of Gases in Multimolecular Layers. *J. Am. Chem. Soc.* **1938**, *60* (2), 309−319.
(45) Richardson, I. G. The calcium silicate hydrates. *Cem. Concr. Res.* **2008**, *38* (2), 137−158.
(46) Myneni, S. C. B.; Traina, S. J.; Logan, T. J. Ettringite solubility and geochemistry of the Ca(OH)2−Al2(SO4)3−H2O system at 1 atm pressure and 298 K. *Chem. Geol.* **1998**, *148* (1−2), 1−19.
(47) Moulder, J. F.; Chastain, J. *Handbook of X-ray Photoelectron Spectroscopy: A Reference Book of Standard Spectra for Identification and Interpretation of XPS Data*; Physical Electronics, PerkinElmer Inc.: Waltham, MA, 1995.
(48) Langmuir, D. *Aqueous Environmental Geochemistry*; Prentice Hall: New York, 1997.
(49) Muftikian, R.; Nebesny, K.; Fernando, Q.; Korte, N. X-ray Photoelectron Spectra of the Palladium−Iron Bimetallic Surface Used for the Rapid Dechlorination of Chlorinated Organic Environmental Contaminants. *Environ. Sci. Technol.* **1996**, *30* (12), 3593−3596.
(50) Fiedor, J. N.; Bostick, W. D.; Jarabek, R. J.; Farrell, J. Understanding the Mechanism of Uranium Removal from Groundwater by Zero-Valent Iron Using X-ray Photoelectron Spectroscopy. *Environ. Sci. Technol.* **1998**, *32* (10), 1466−1473.
(51) Grossl, P. R.; Eick, M.; Sparks, D. L.; Goldberg, S.; Ainsworth, C. C. Arsenate and Chromate Retention Mechanisms on Goethite. 2. Kinetic Evaluation Using a Pressure-Jump Relaxation Technique. *Environ. Sci. Technol.* **1997**, *31* (2), 321−326.
(52) Fendorf, S.; Eick, M. J.; Grossl, P.; Sparks, D. L. Arsenate and Chromate Retention Mechanisms on Goethite. 1. Surface Structure. *Environ. Sci. Technol.* **1997**, *31* (2), 315−320.
(53) Singer, D. M.; Chatman, S. M.; Ilton, E. S.; Rosso, K. M.; Banfield, J. F.; Waychunas, G. A. Identification of Simultaneous U(VI) Sorption Complexes and U(IV) Nanoprecipitates on the Magnetite (111) Surface. *Environ. Sci. Technol.* **2012**, *46* (7), 3811−3820.
(54) Silva, R. J. N. H. Actinide Environmental Chemistry. *Radiochim. Acta* **1995**, *70/71*, 377−396.
(55) Thorpe, C. L.; Lloyd, J. R.; Law, G. T. W.; Burke, I. T.; Shaw, S.; Bryan, N. D.; Morris, K. Strontium sorption and precipitation behaviour during bioreduction in nitrate impacted sediments. *Chem. Geol.* **2012**, *306−307*, 114−122.
(56) Pratt, A. R.; Blowes, D. W.; Ptacek, C. J. Products of Chromate Reduction on Proposed Subsurface Remediation Material. *Environ. Sci. Technol.* **1997**, *31* (9), 2492−2498.
(57) Wilkin, R. T.; Su, C.; Ford, R. G.; Paul, C. J. Chromium-Removal Processes during Groundwater Remediation by a Zerovalent Iron Permeable Reactive Barrier. *Environ. Sci. Technol.* **2005**, *39* (12), 4599−4605.
(58) Small, T. D.; Warren, L. A.; Roden, E. E.; Ferris, F. G. Sorption of Strontium by Bacteria, Fe(III) Oxide, and Bacteria−Fe(III) Oxide Composites. *Environ. Sci. Technol.* **1999**, *33* (24), 4465−4470.
(59) Lehrman, L.; Shuldener, H. L. Action of Sodium Silicate as a Corrosion Inhibitor in Water Piping. *Ind. Eng. Chem.* **1952**, *44* (8), 1765−1769.
(60) Lahodny-Sarc, O.; Kastelan, L. The influence of pH on the inhibition of corrosion of iron and mild steel by sodium silicate. *Corros. Sci.* **1981**, *21* (4), 265−271.
(61) Brito, F.; Ascanio, J.; Mateo, S.; Hernández, C.; Araujo, L.; Gili, P.; Martín-Zarza, P.; Domínguez, S.; Mederos, A. Equilibria of chromate(VI) species in acid medium and ab initio studies of these species. *Polyhedron* **1997**, *16* (21), 3835−3846.
(62) Wilkin, R. T.; Puls, R. W.; Sewell, G. W. Long-Term Performance of Permeable Reactive Barriers Using Zero-Valent Iron: Geochemical and Microbiological Effects. *Ground Water* **2003**, *41* (4), 493−503.
(63) Csovari, M.; Csicsak, J.; Folding, G.; Simoncsics, G. Experimental iron barrier in Pecs, Hungary. In *Long-Term Performance of Permeable Reactive Barriers*; Roehl, K. E., Meggyes, T., Simon, F. G., Stewart, D. I., Eds.; Elsevier: New York, 2005.